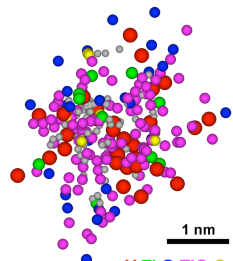


A Multiscale Approach to Developing and Predicting the Behavior of High Performance Materials for Advanced Nuclear Energy Systems



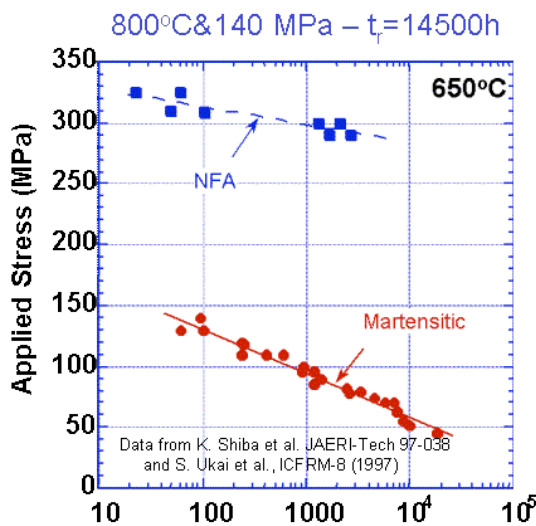
G. R. Odette¹, M. J. Alinger^{1,a},
B.D. Wirth² and M. K. Miller³

¹Materials Department, University of California Santa Barbara

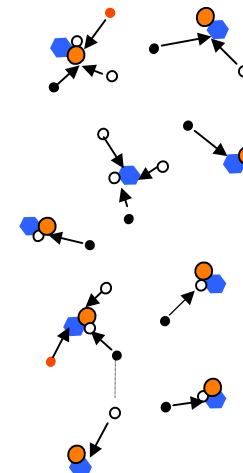
²Nuclear Engineering Department, University of California Berkeley

³ Materials Science Division, ORNL

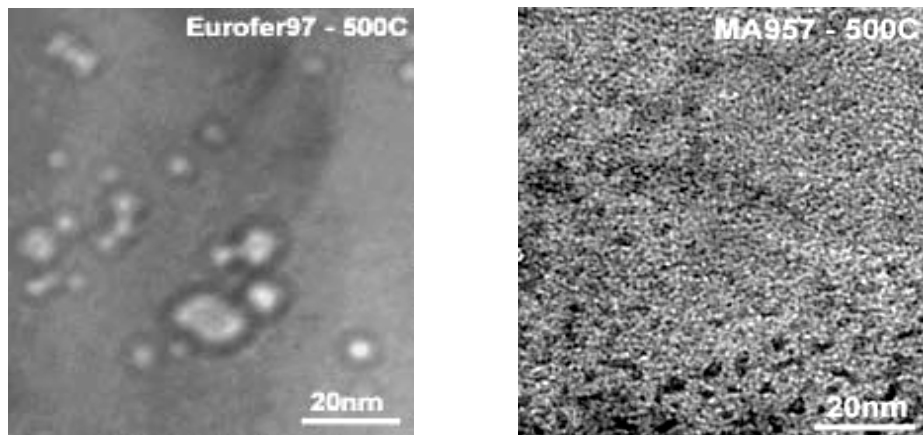
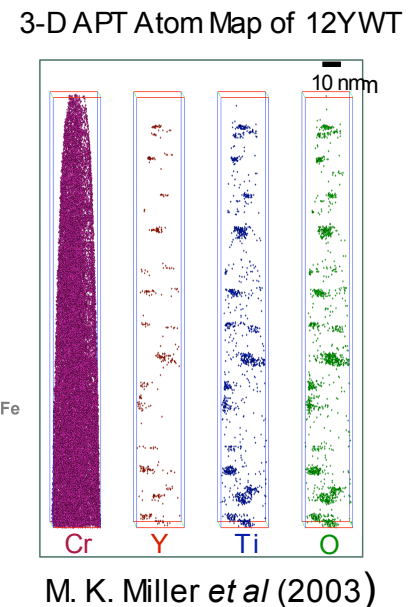
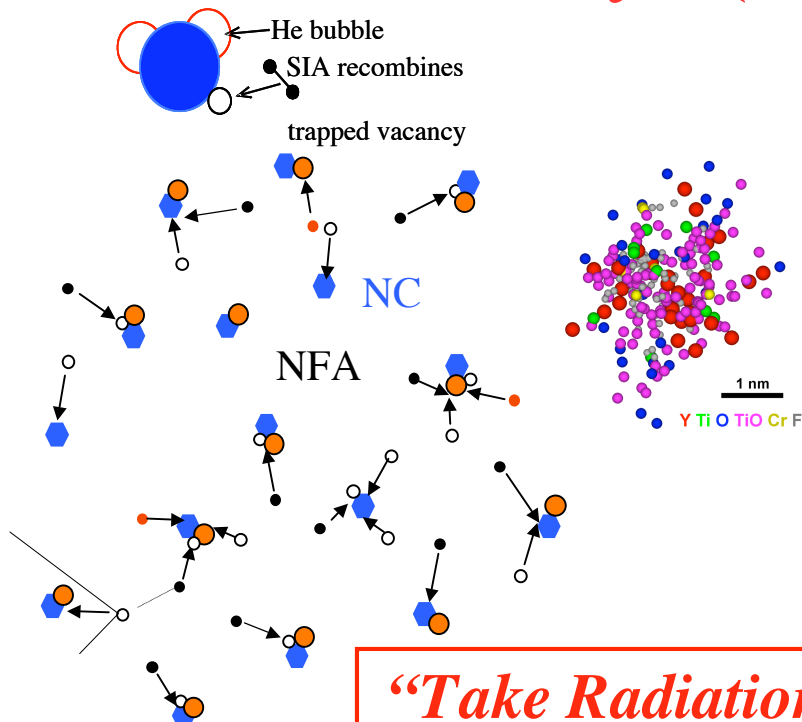
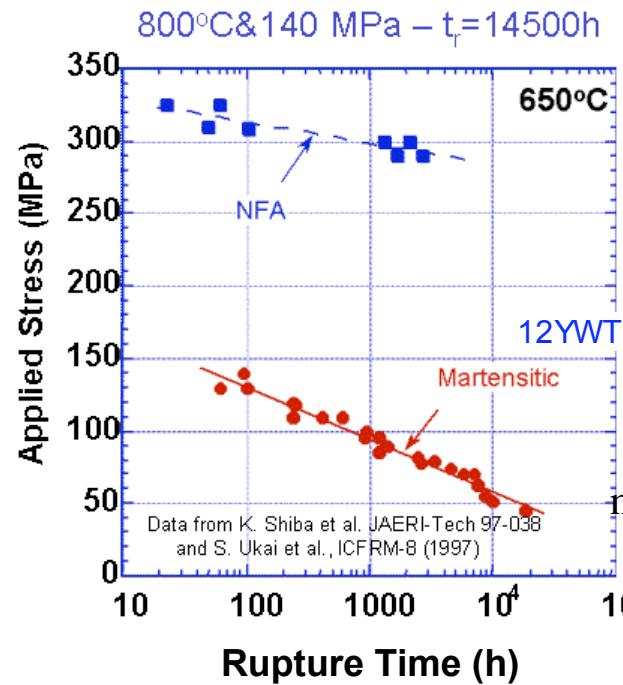
a. Currently at GE Corporate Research



**ICMR Summer Program on
Advanced Thermostructural Materials
UCSB, 15 August 2006**



Nanostructured Ferritic Alloys (NFAs)



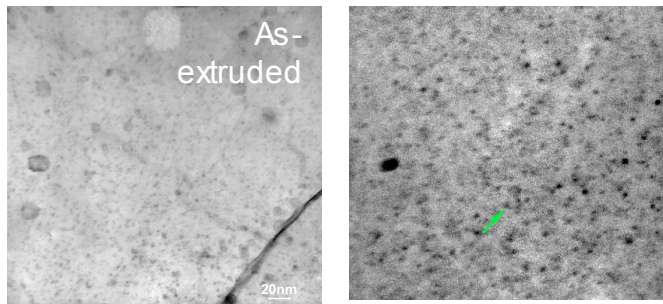
Helium bubbles in Eurofer97 and MA957

“Take Radiation Damage off the Table”

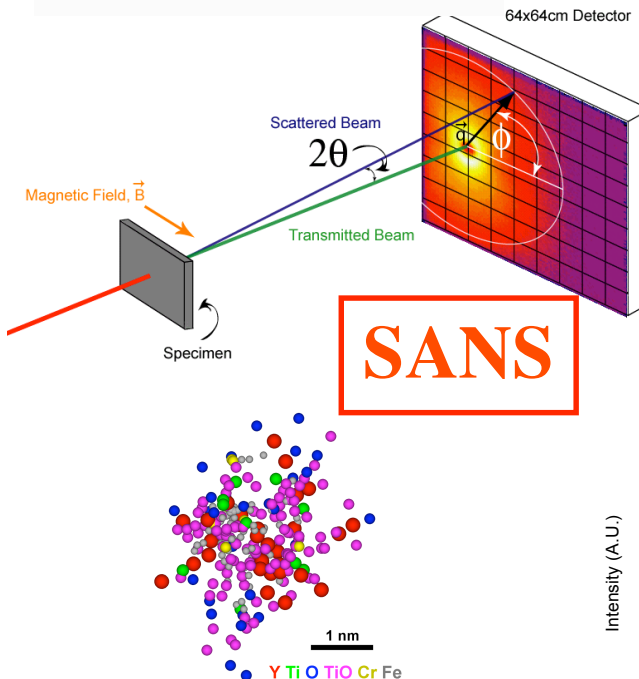
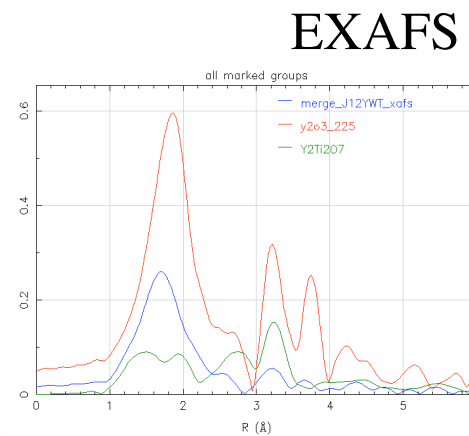
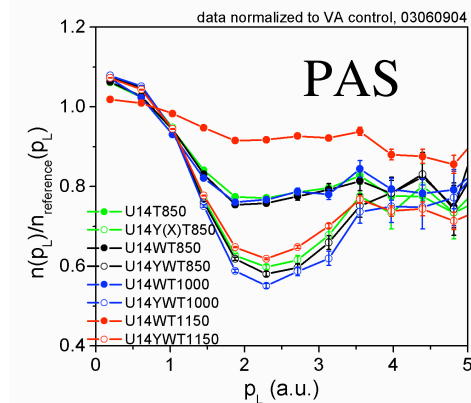
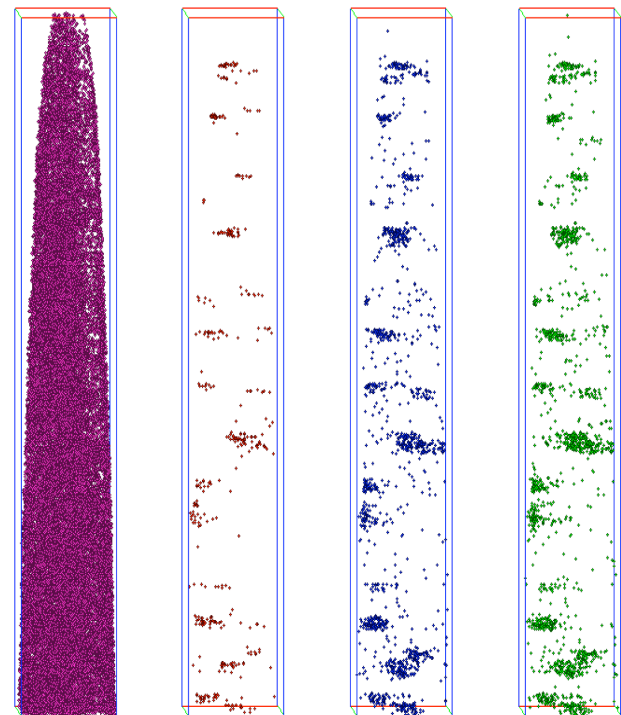
Operate $> 0.5T_m$ with high trap densities to recombine vacancies and SIA/manage helium by trapping in fine nm-scale high pressure bubbles

Characterization Techniques Are Key

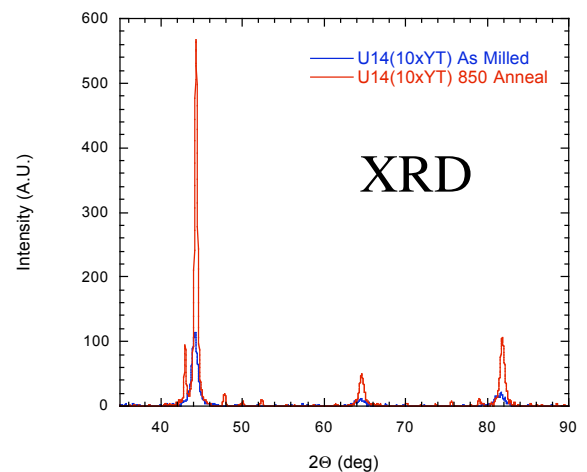
TEM and EFTEM



3-D APT



SANS



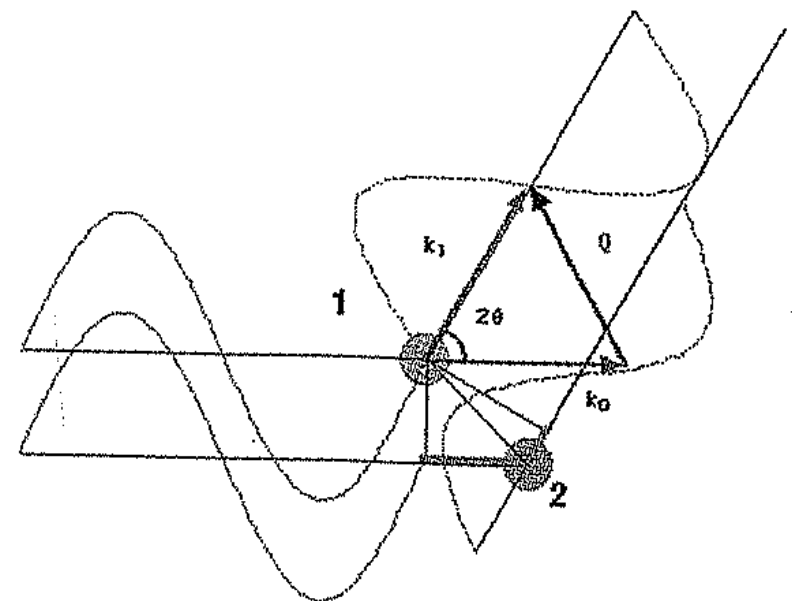
Small Angle Neutron Scattering (SANS)

SANS is the result of coherent elastic diffraction at small angles around a beam of thermal or cold neutrons by features (precipitates, solute clusters, defects) with different scattering length (nuclear and magnetic) densities (ρ) than the matrix they are embedded in

$$\rho_{p/m} = \sum_{ip/m} [N_{at}/V] X_i b_i$$

Here b_i = scattering length for isotopes in the matrix (m) and feature (p)

The measurable size (r) range of the features is bigger than atoms and smaller than ... (1-100 nm)



$$d\Sigma/dq = V^{-1} \sum_{i,j} b_i b_j \exp[iq(r_i - r_j)]$$

Small Angle Neutron Scattering (SANS)

SANS is quantified as a cross section - $d\Sigma/d\Omega(\mathbf{q})$ - that varies with the scattering vector (\mathbf{q}) - for a neutron with wavelength λ at scattering at angle 2θ -

$$q = 4\pi \sin(\theta)/\lambda$$

In the case of dilute (non-interacting) features $d\Sigma/d\Omega(\mathbf{q})$ depends the size (r_p), volume fraction (f_p) and volume (V_p) of the feature and it's ρ contrast with the matrix $\Delta\rho = (\rho_p - \rho_m)$

$$d\Sigma/d\Omega(\mathbf{q}) = f_p V_p \Delta\rho^2 [F_p(qr)]^2$$

Here $F(q)$ is a shape-dependent form factor that depends on r - i.e. for a sphere

$$F_p(q) = \{3[\sin(qr_p) - qr_p \cos(qr_p)]/[qr_p]^3\}$$

Shapes Scattering Curves

Single type/size feature - the normalized $d\Sigma/d\Omega(q)/d\Sigma/d\Omega(0) = d\Sigma/d\Omega(q)_n$ determined by $r_p \rightarrow$ plot $\log[d\Sigma/d\Omega(q)_n]$ vs. q^2

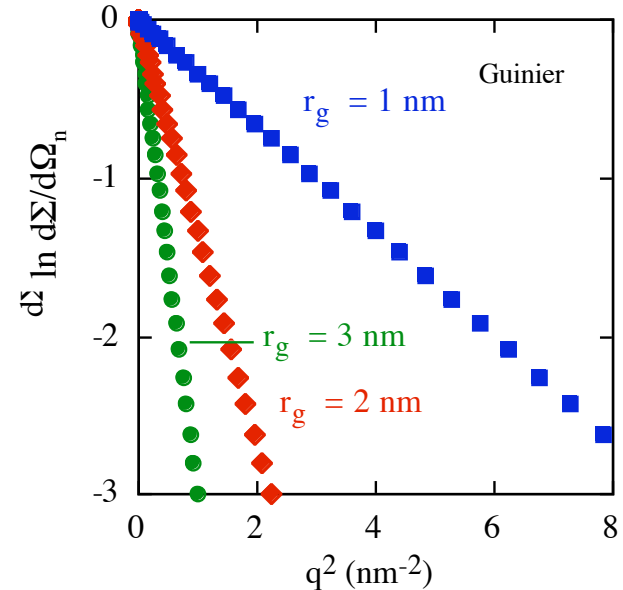
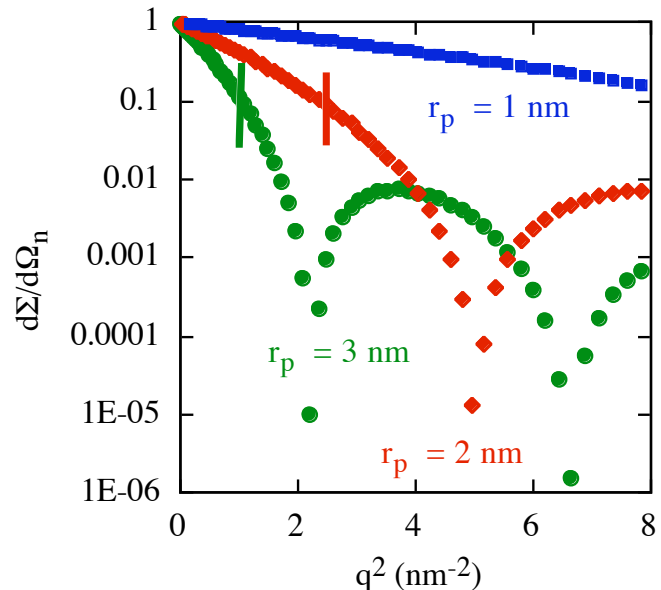
For $qr_p < \approx 3$ Guinier approximation \rightarrow

$$d\Sigma/d\Omega(q)_n \approx \exp[-(qr_g)^2/3]$$

Can fit $d\Sigma/d\Omega(q)_n$ data to find $r_p \rightarrow$

$$\ln[d\Sigma/d\Omega(q)_n] = -[r_g^2/3]q^2 \rightarrow r_p = \sqrt{(5/3)r_g}$$

Small nm-scale features scatter at higher q and are thus easily detected in many materials



Details, Absolute Fits and Complications

Reduce raw count data from a 2D position sensitive detector to establish a measured feature $I_p(q)$ (usually using a control) - absolute $d\Sigma/d\Omega(q)_p$ based on a calibration standard

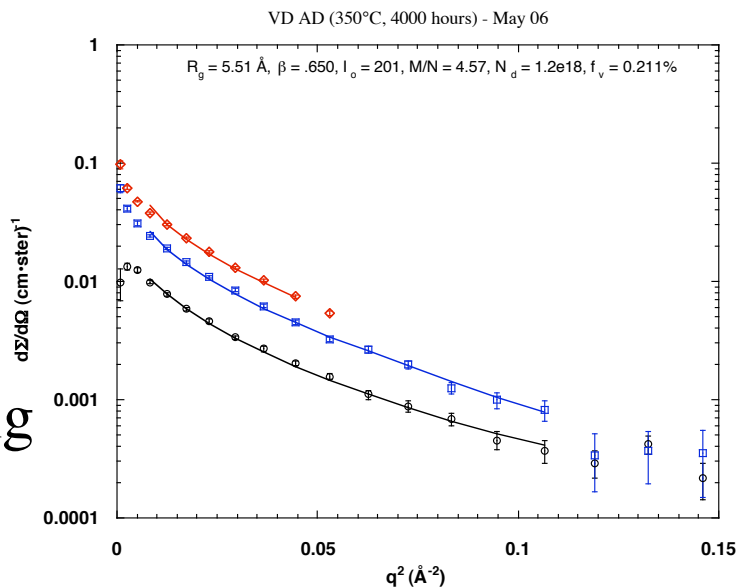
Particle size distributions smears out $d\Sigma/d\Omega(q)_p$ curves \rightarrow fit distribution functions like *ln normal* - note distributions (narrow?) of λ and resolution limits also smear out $d\Sigma/d\Omega(q)$

Fit absolute $d\Sigma/d\Omega(q)_p$ to establish feature number densities (N_p) - volume fractions (f_p) - size distributions ($\langle r_p \rangle$, β)

Need to know $\Delta\rho = (\rho_p - \rho_m)$

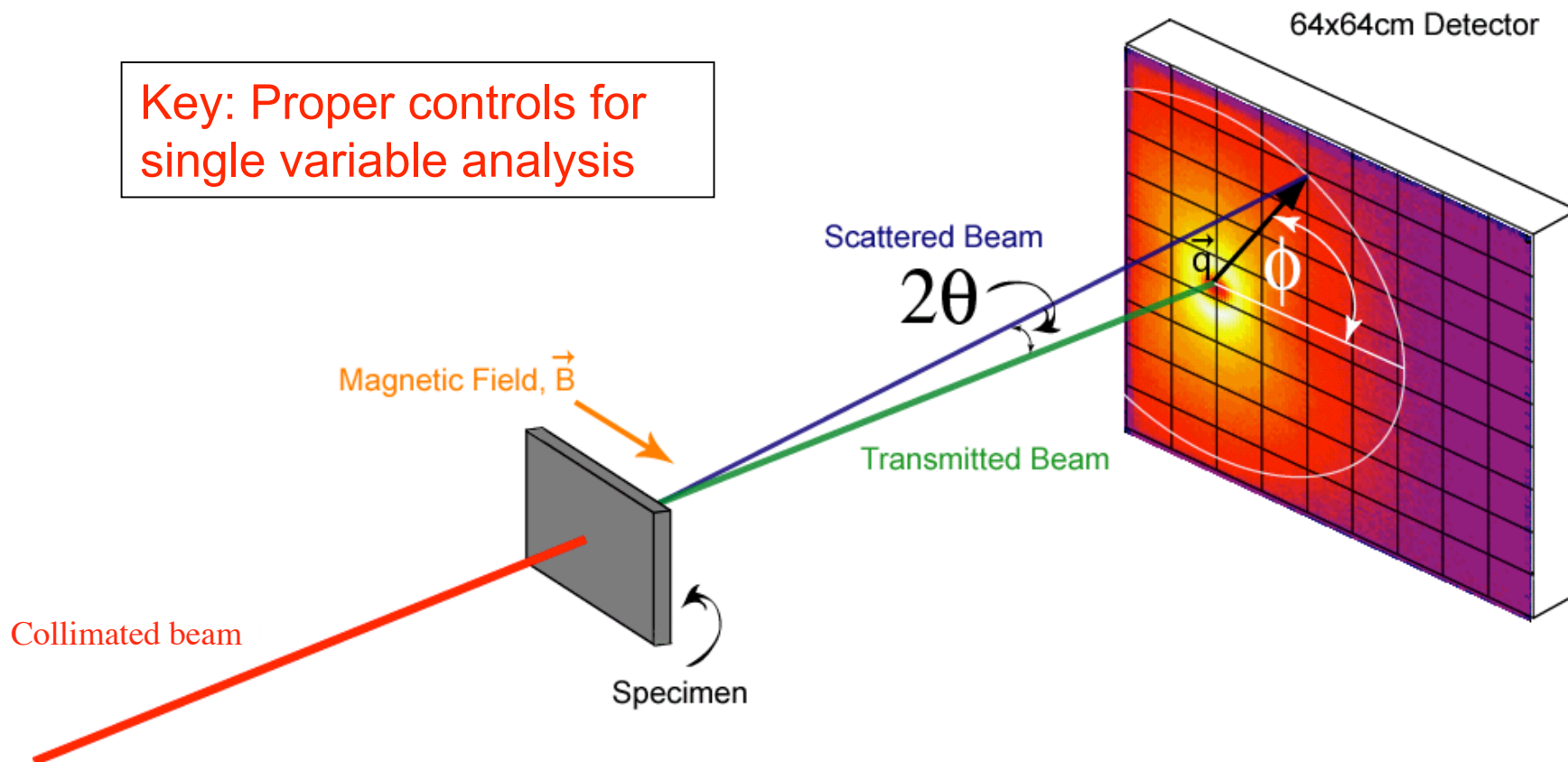
Multiple features add complications

Exploit magnetic and nuclear scattering
 $\rightarrow d\Sigma/d\Omega(q)_{pm}$ and $d\Sigma/d\Omega(q)_{pn}$



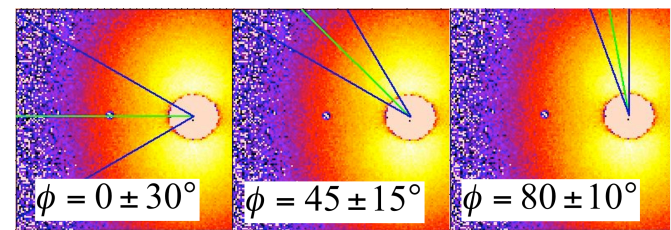
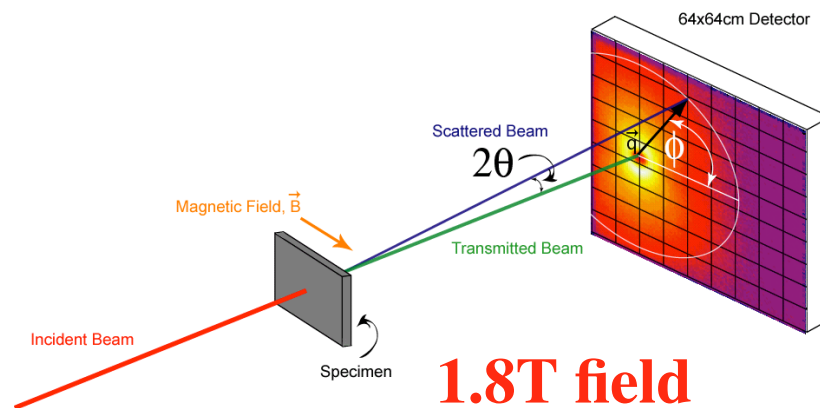
Experimental Configuration (NIST)

- NIST CNR NG1 and NG7
- Measure nuclear & magnetic scattering in 1.8T B-field
- Corrected sample scattering minus **control** with H₂O standard



Nuclear and Magnetic Scattering

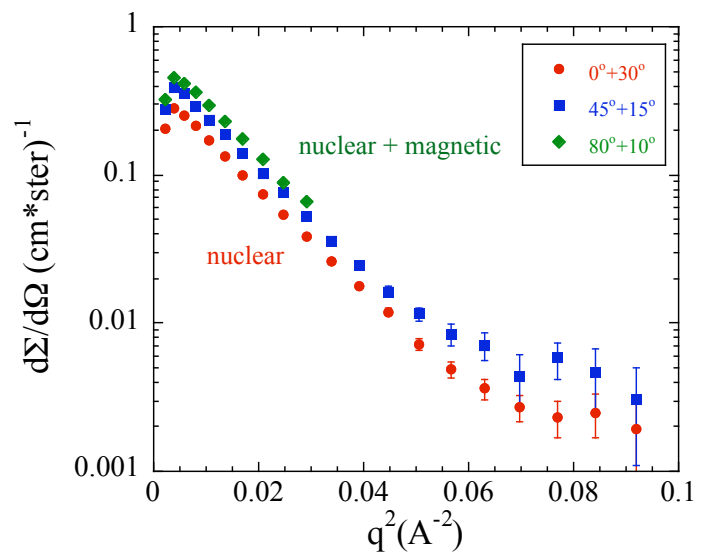
$$\frac{d\Sigma(q)}{d\Omega} = \frac{d\Sigma_{nuc}(q)}{d\Omega} + \frac{\sin^2 \phi}{\sin^2 \theta} \frac{d\Sigma_{mag}(q)}{d\Omega}$$



$$q = \frac{4\pi \sin(\theta)}{\lambda} [matrix - feature\ contrast\ factor]^2$$

$$kI(q, \phi) = \frac{d\Sigma(q, \phi)}{d\Omega} = NV^2 \Delta\rho^2 F(qr)$$

Number density Volume radius form factor



Fitting

Fit log-normal distribution to $d\Sigma/d\Omega$

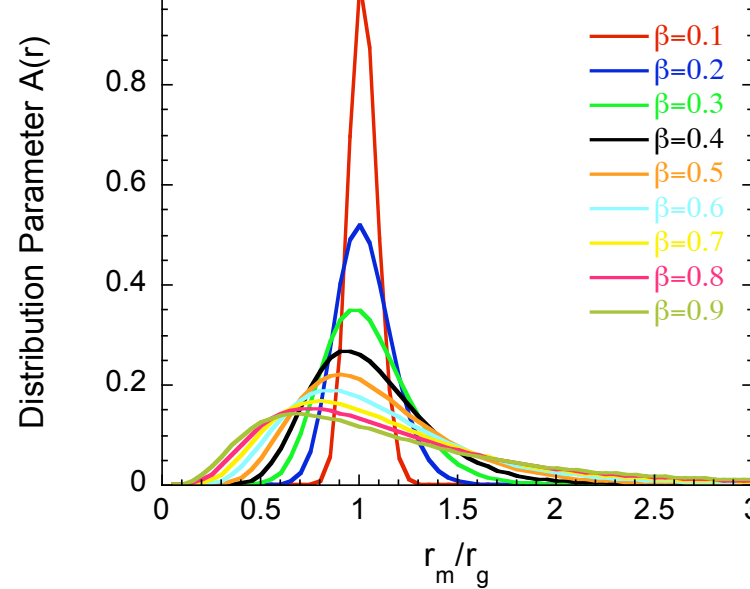
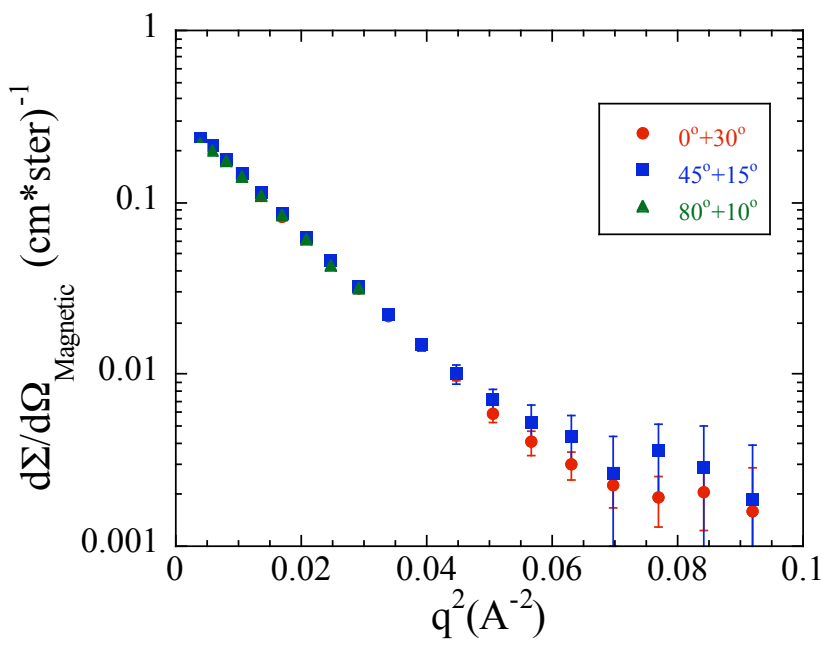
$$\langle r^3 \rangle^{1/3} = r_m \exp(0.75\beta^2)$$

$$f_p = (3/4\pi) (\exp(-6.75\beta^2)) (\Delta\rho^{-2} r_m^{-3}) (d\Sigma_{\text{mag}}(0)/d\Omega)$$

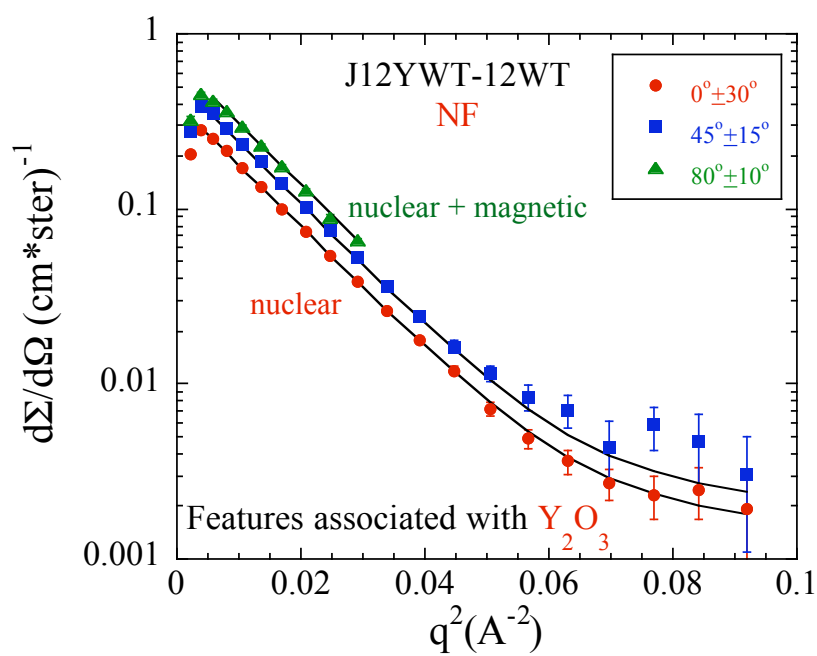
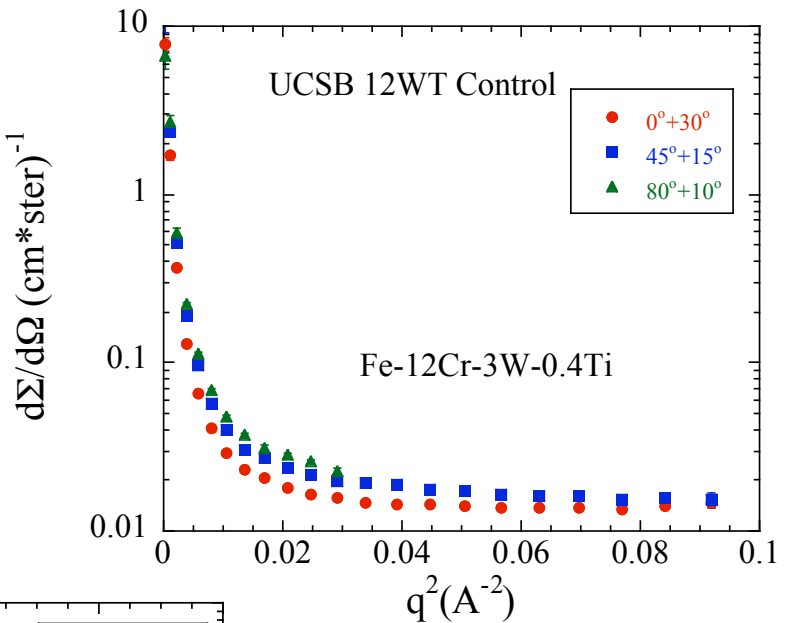
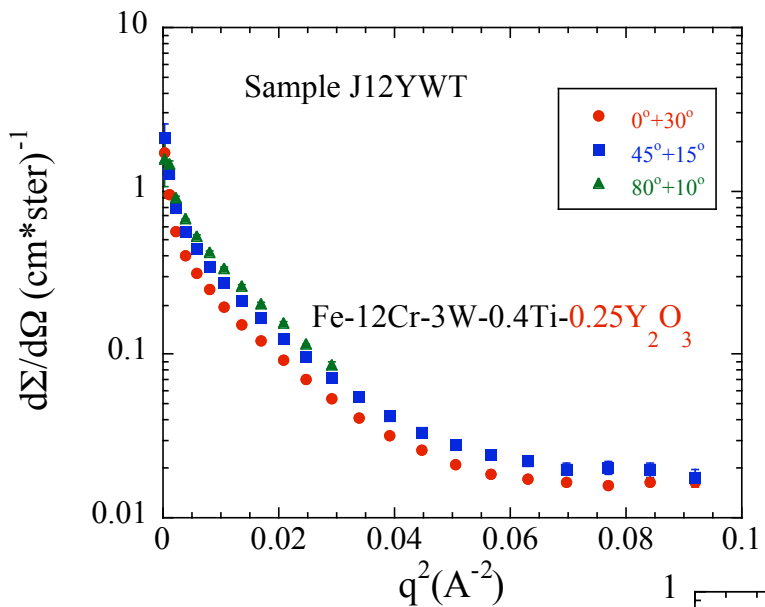
non-magnetic hole in saturated Fe matrix

$$N_p = (3/4\pi)^2 (\exp(-9\beta^2)) (\Delta\rho^{-2} r_m^{-6}) (d\Sigma_{\text{mag}}(0)/d\Omega)$$

variables to be fit



Example - J12YWT



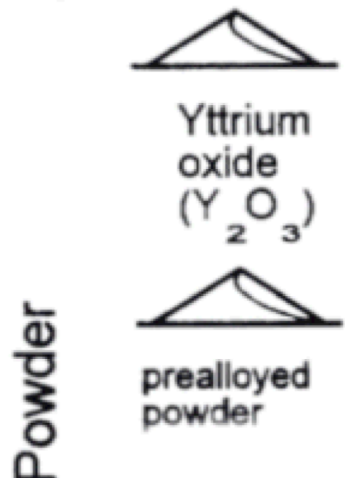
$$r = 1.61 \text{ nm}$$

$$f = 0.69 \%$$

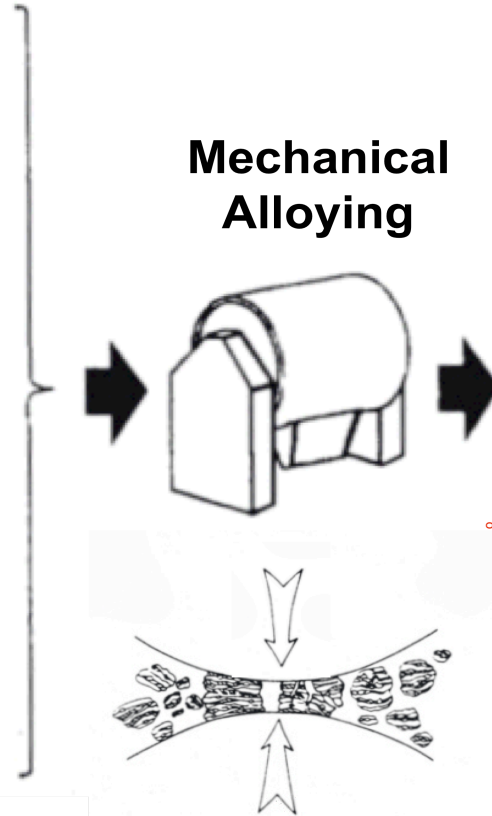
$$N = 0.39 \times 10^{24}/\text{m}^3$$

NFA Processing Steps

Prepare (acquire)
high quality
(purity) powders -
Fe-Cr alloys and
 Y_2O_3



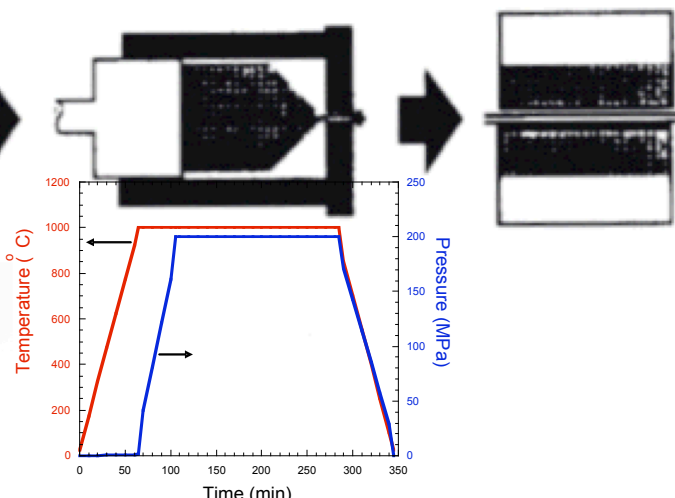
Mechanically
alloy powders by
ball milling



Consolidate
milled powders by
a process like
HIPing or hot
extrusion

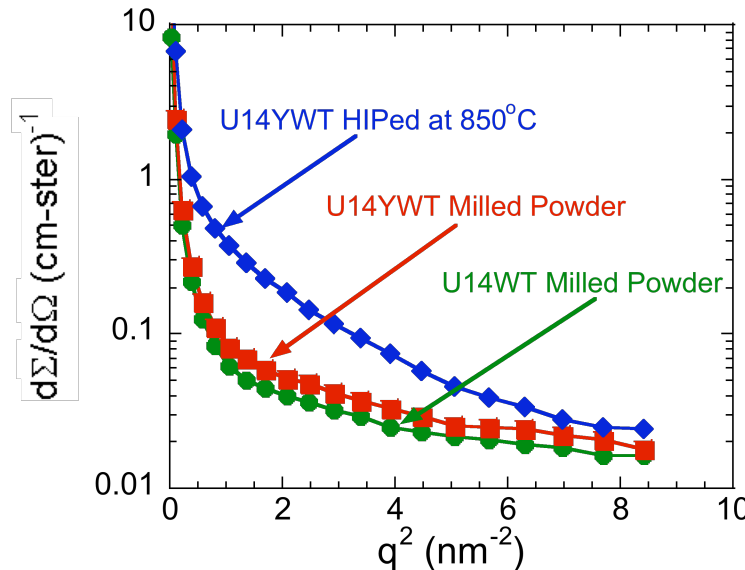
**Thermo-Mechanical
Processing**

**Hot
Consolidation**



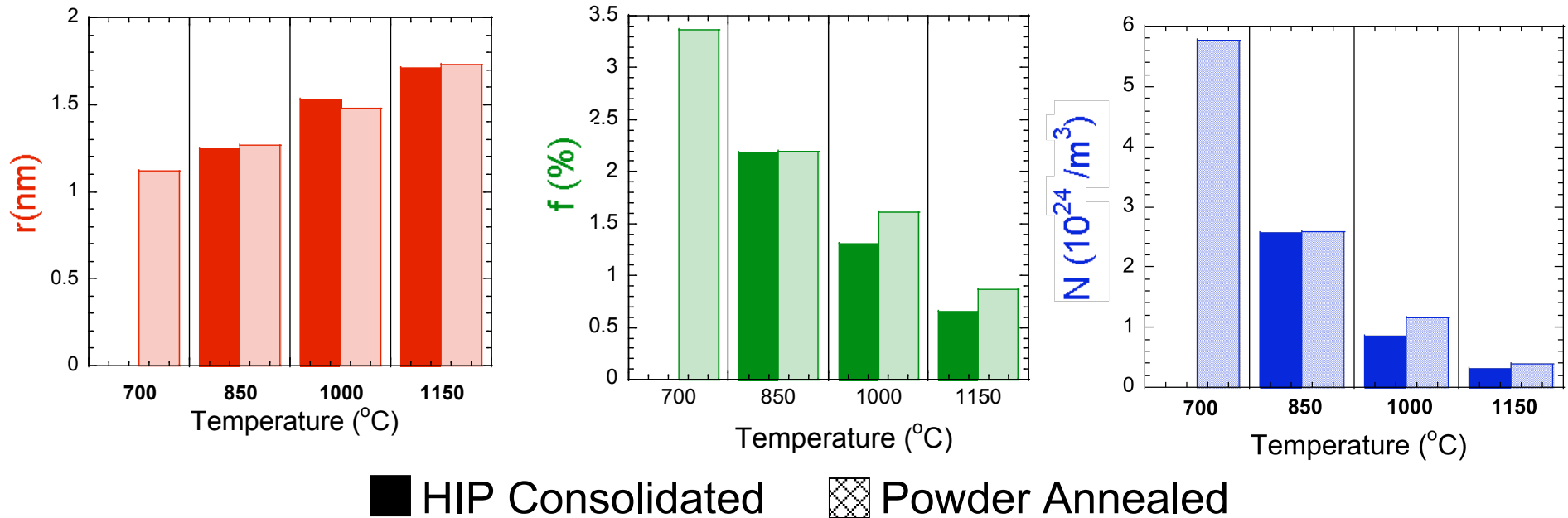
Post-consolidation
processes like
recovery and
recrystallization
annealing

What Happens to Y_2O_3 during MA?



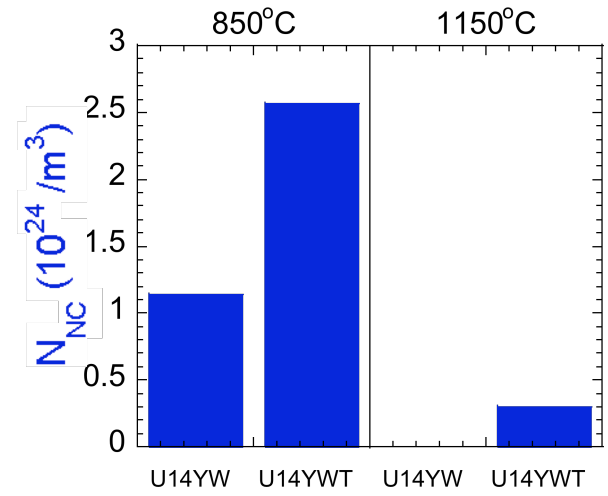
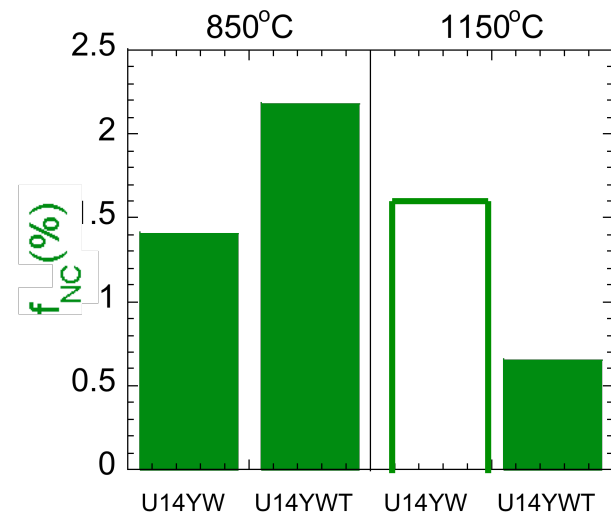
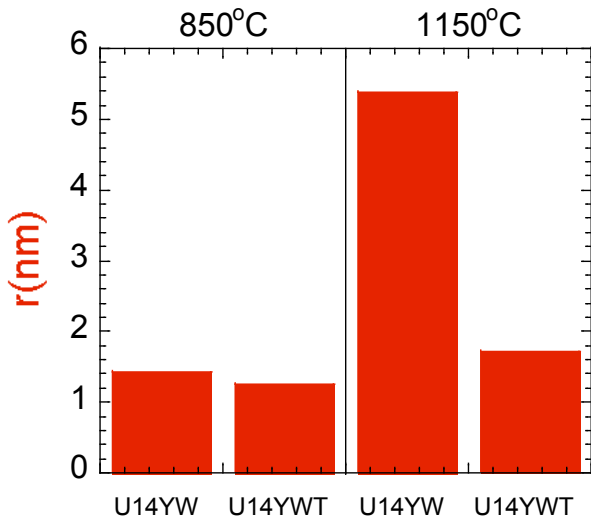
- SANS and other measurements on powders shows mechanical alloying dissolves most of the Y_2O_3 - control and milled samples scattering are \approx same.
- NCs with $r = 1$ to 2 nm features form during high temperature consolidation

What Controls the NCs r, N and f?



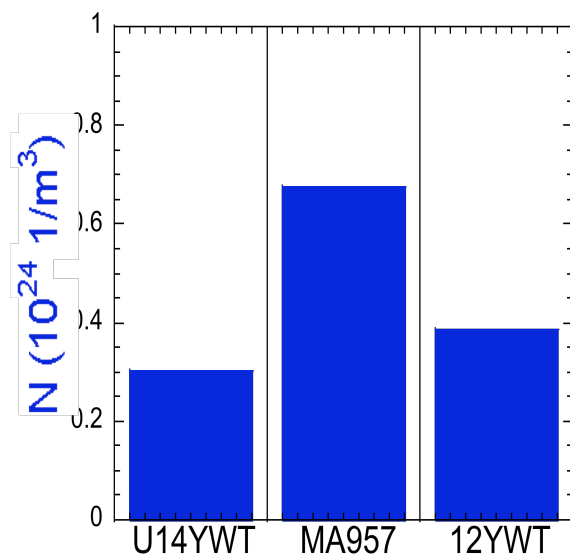
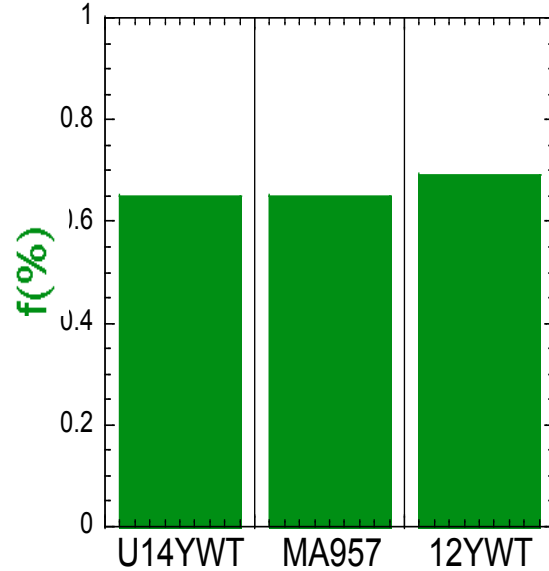
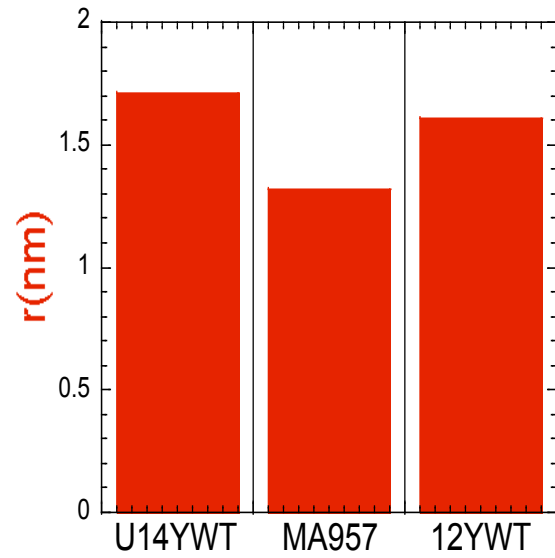
- The NCs r increase while number density (N) and volume fraction (f) decrease with increasing HIPing temperature
- HIP consolidation and direct powder annealing for same t-T history produce very similar NCs

Necessary Ingredients for NCs?



- Y, Ti and high energy (SPEX versus attritor) milling produce a larger f for HIPing at 850°C and both seem necessary at 1150°C

Model Versus INCO and Kobe Alloys

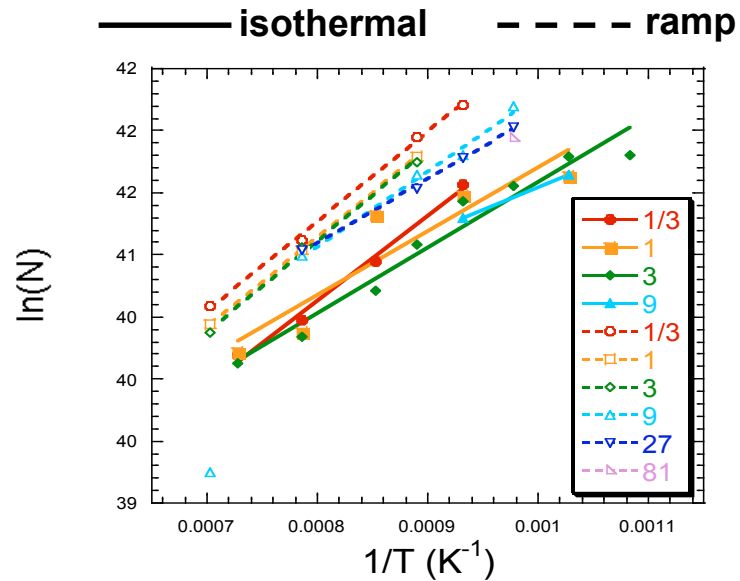
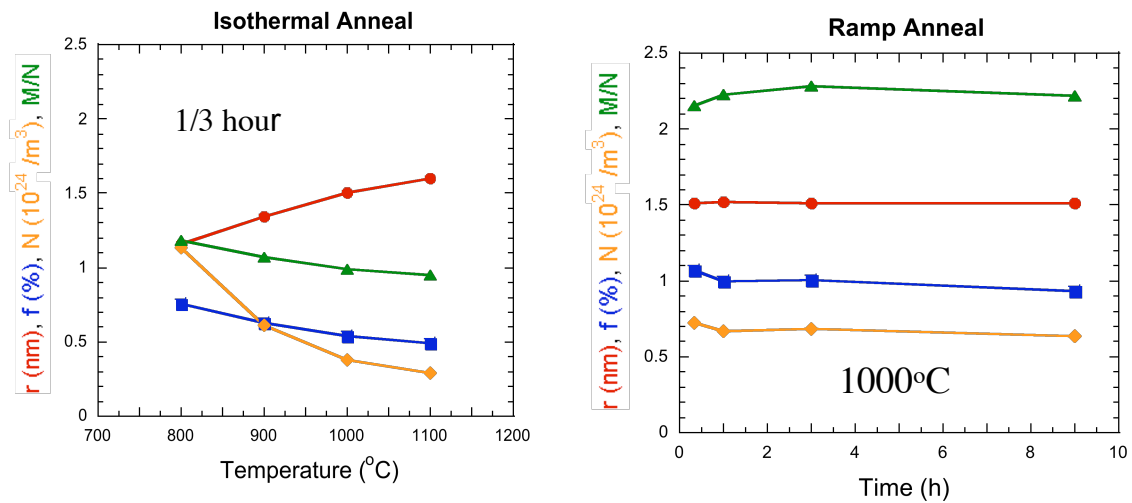


- UCSB model alloys and J12WYT and MA957 contain similar NCs

NC Precipitation Kinetics

NF precipitation kinetics (SANS)

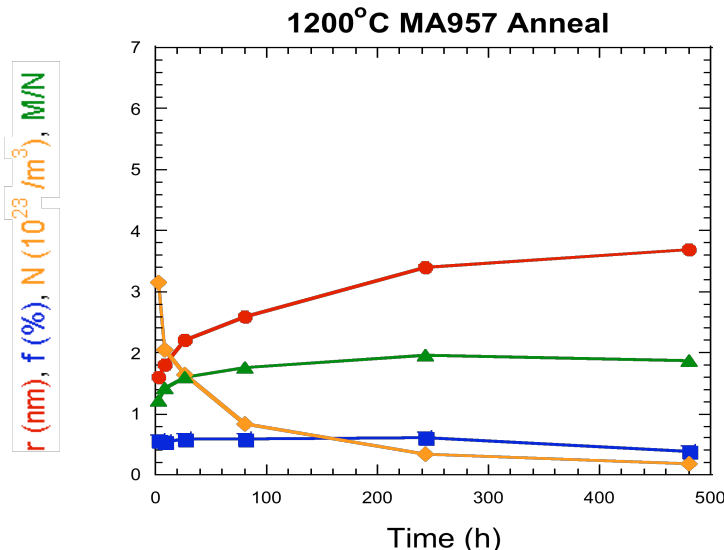
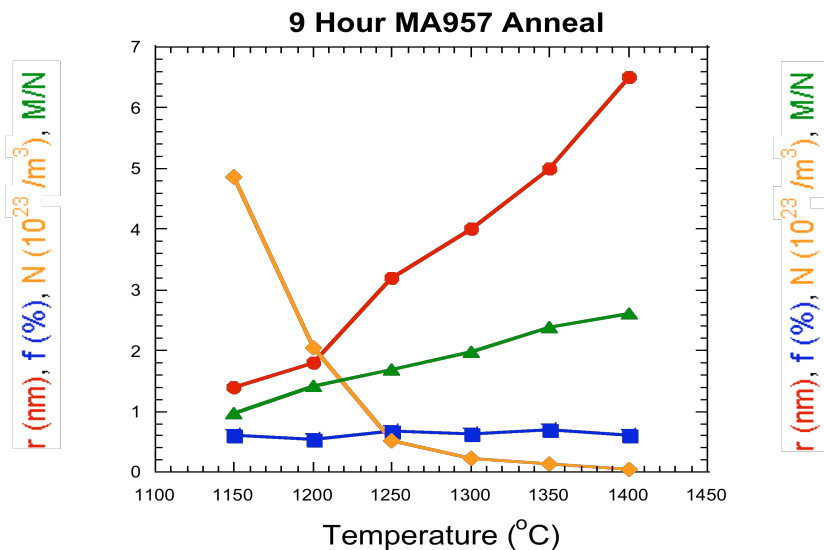
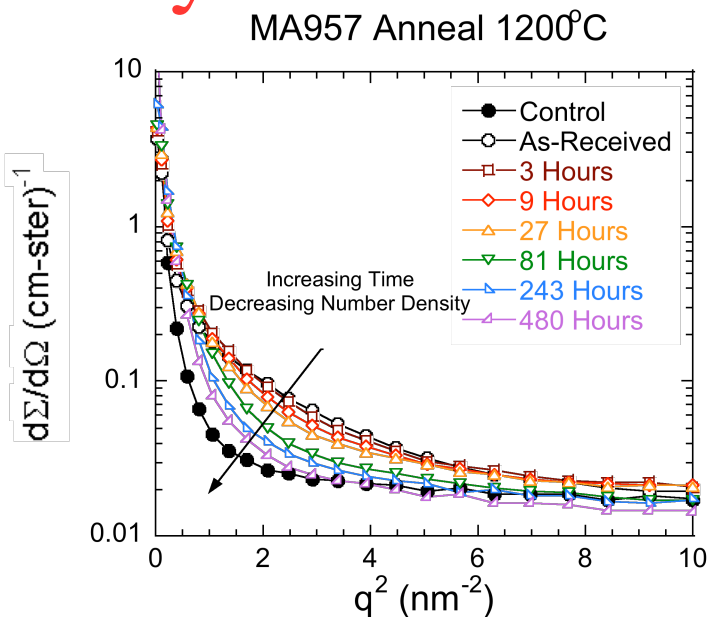
Temperature (°C)	ramp rate	Time (hours)				
		1/3	1	3	9	27
650	ramp					
650	isothermal		X			
650	ramp					
700	isothermal	X	X	X		
700	ramp				X	X
750	isothermal		X			
750	ramp	X			X	X
800	isothermal	X	X	X	X	
800	ramp	X	X	X	X	X
850	isothermal			X		
850	ramp					
900	isothermal	X	X	X		
900	ramp	X	X	X	X	X
1000	isothermal	X	X	X		
1000	ramp	X	X	X	X	X
1100	isothermal	X	X	X		
1100	ramp	X	X	X	X	
1150	isothermal					



Are NCs Thermally Stable?

- MA957 - extruded at 1150°C

Temperature (°C)	Time (hours)							
	1/3	1	3	9	27	81	243	480
1150			X	X	X	X	X	X
1175			X		X		X	X
1200			X	X	X	X	X	X
1225	X		X		X		X	
1250	X	X	X	X	X	X	X	
1300			X	X	X			
1350			X	X	X			
1400			X	X				

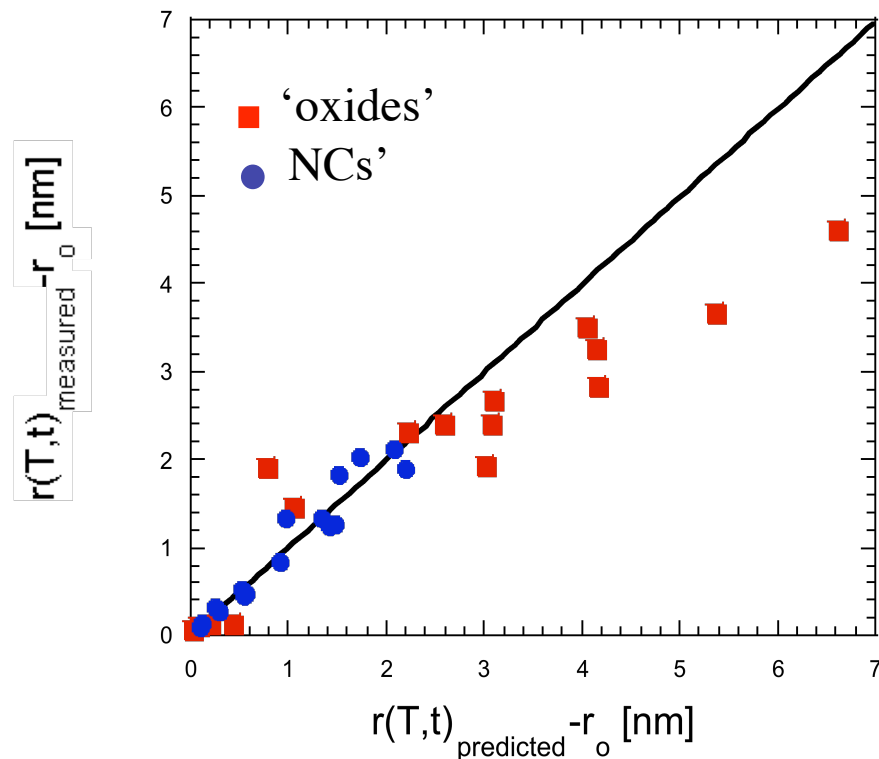


Pipe Diffusion Coarsening Model

- Dislocation pipe diffusion ($r^5 \propto t$)

$$r(t_a, T_a) - r_o \approx r_o [2.4 \times 10^{27} \exp(-880000/RT) - 1]^{1/5}$$

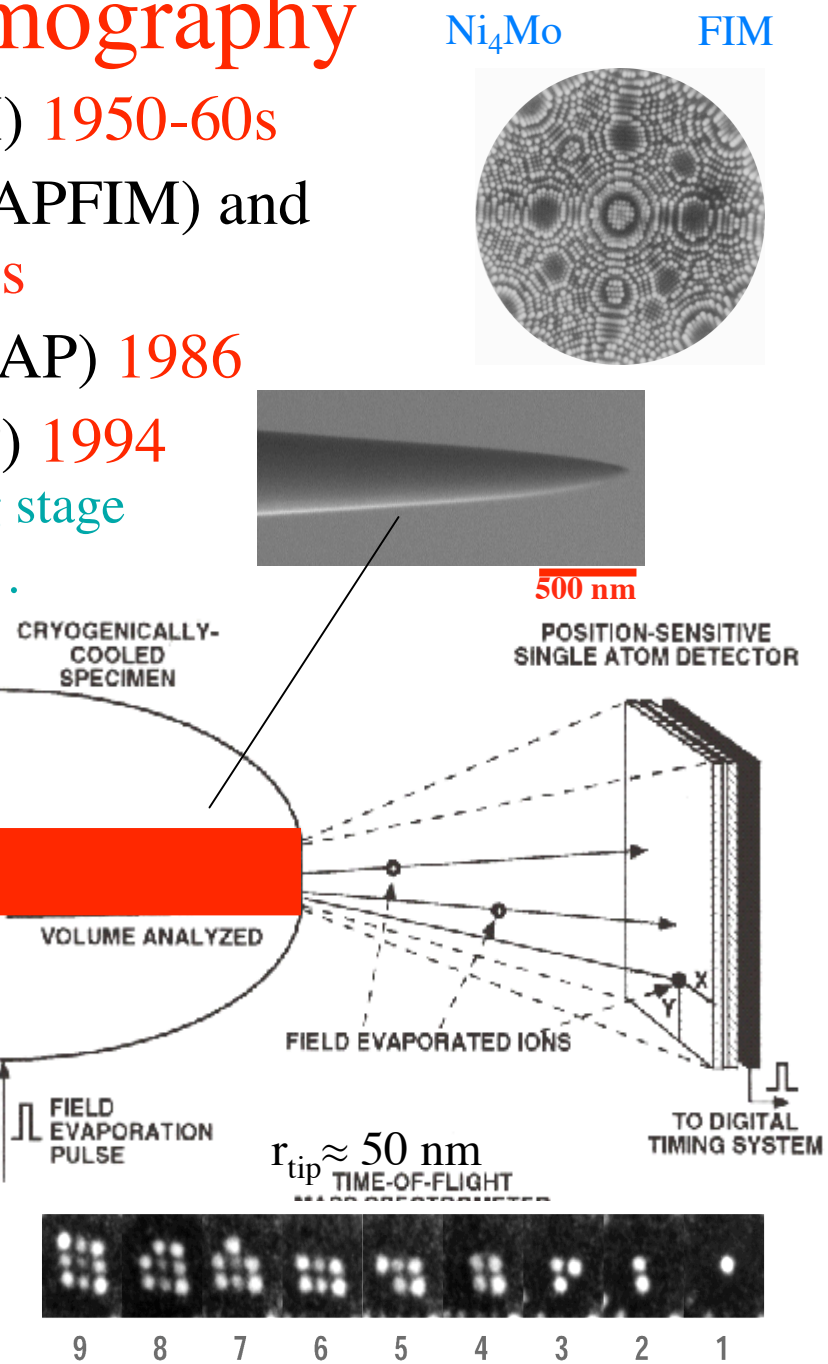
- NC transform to nearer-equilibrium oxide phases at $r \approx 3.5\text{nm}$



Slight coarsening
@ 1000°C/3000h
 $\langle r \rangle \approx 2 \rightarrow 3\text{nm}$
(TEM)

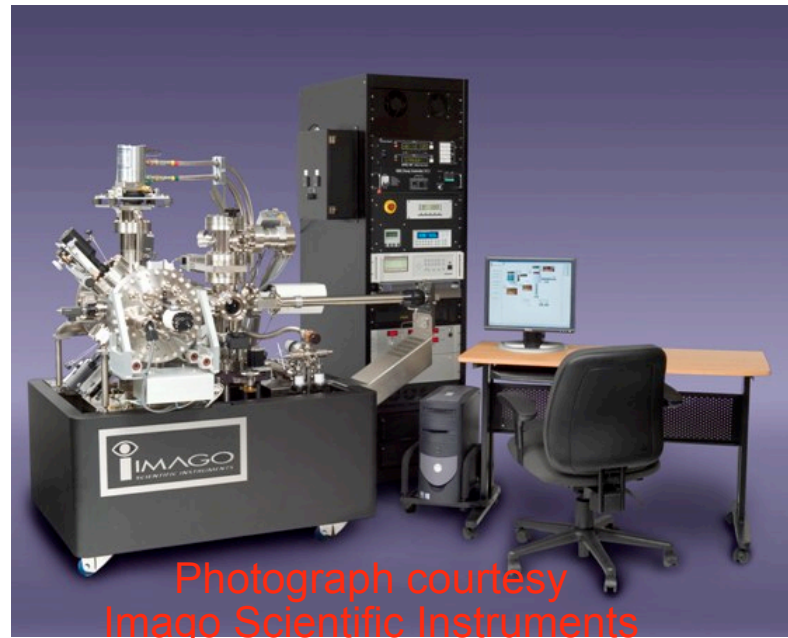
Atom Probe Tomography

- Roots in Field Ion Microscope (FIM) 1950-60s
- Atom Probe Field Ion Microscope (APFIM) and Imaging Atom Probe (IAP) 1970-80s
- Three-dimensional Atom Probe (3DAP) 1986
- Local Electrode Atom Probe (LEAP) 1994
 - local electrode on XYZ nanopositioning stage
 - three-dimensional element atom maps ...
 - commercial introduction 2003
 - laser pulsing - 2006
- Layer-by-layer atom evaporation in high specimen tip field by voltage pulses ($\approx 1/50$) -> back track trajectories to measure atom position with a 2D detector
- Reconstruct 3D nanostructures



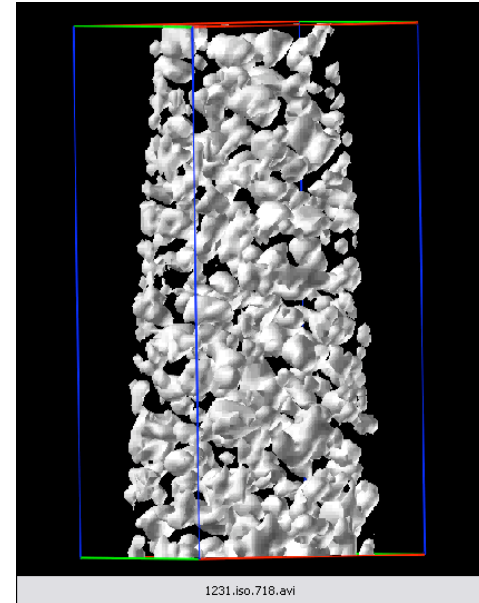
State-of-the-Art Local Electrode Atom Probe

γ''/γ'' precipitates in Alloy 718

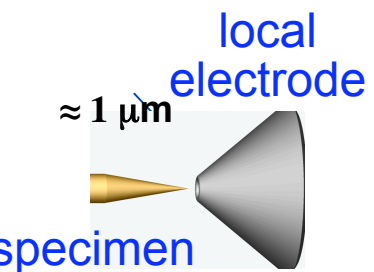


Photograph courtesy
Imago Scientific Instruments

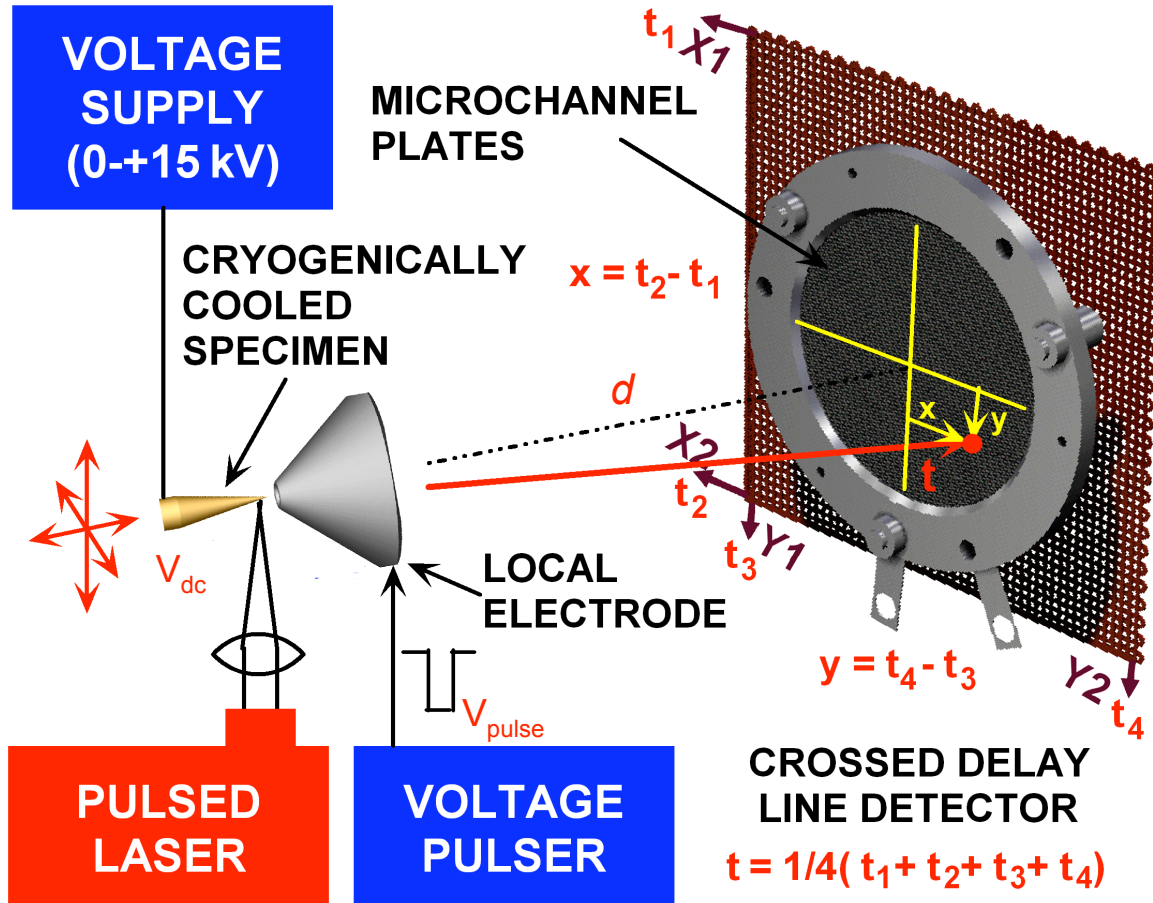
11.4 M
atoms in
 ~ 1 h



Improved detector and stage design, high speed
pulse generators and digital timing systems ->
shorter experiments (days to minutes - 300x)
significantly more atoms (to >100 million atoms)
larger fields of view (40x improvement)



Local Electrode Atom Probe



The mass-to-charge ratio is derived from the flight time, t , and applied voltages, V_{dc} and V_{pulse}

$$\frac{m}{n} = c \left(V_{dc} + \alpha V_{pulse} \right) \frac{t^2}{d^2}$$

x - y coordinates from detector impact position

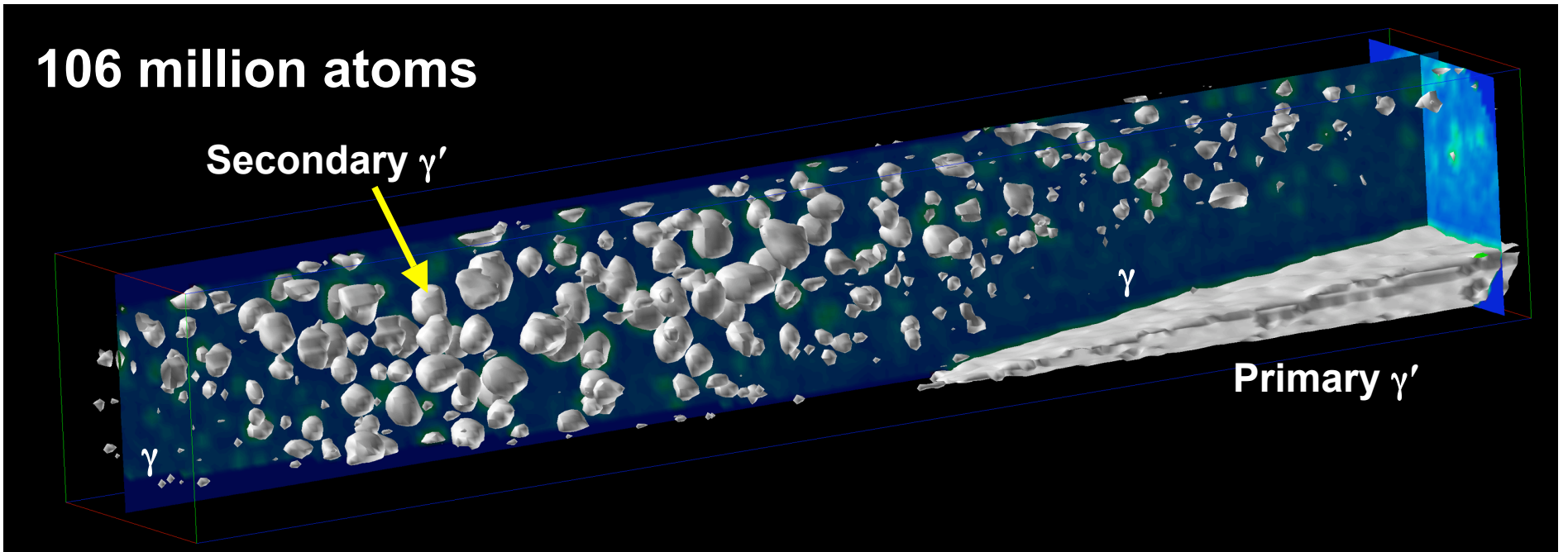
z coordinate determined from position in the evaporation sequence

Potential Energy → Kinetic Energy
 $neE = \frac{1}{2}mv^2$

Data are reconstructed into 3D volumes

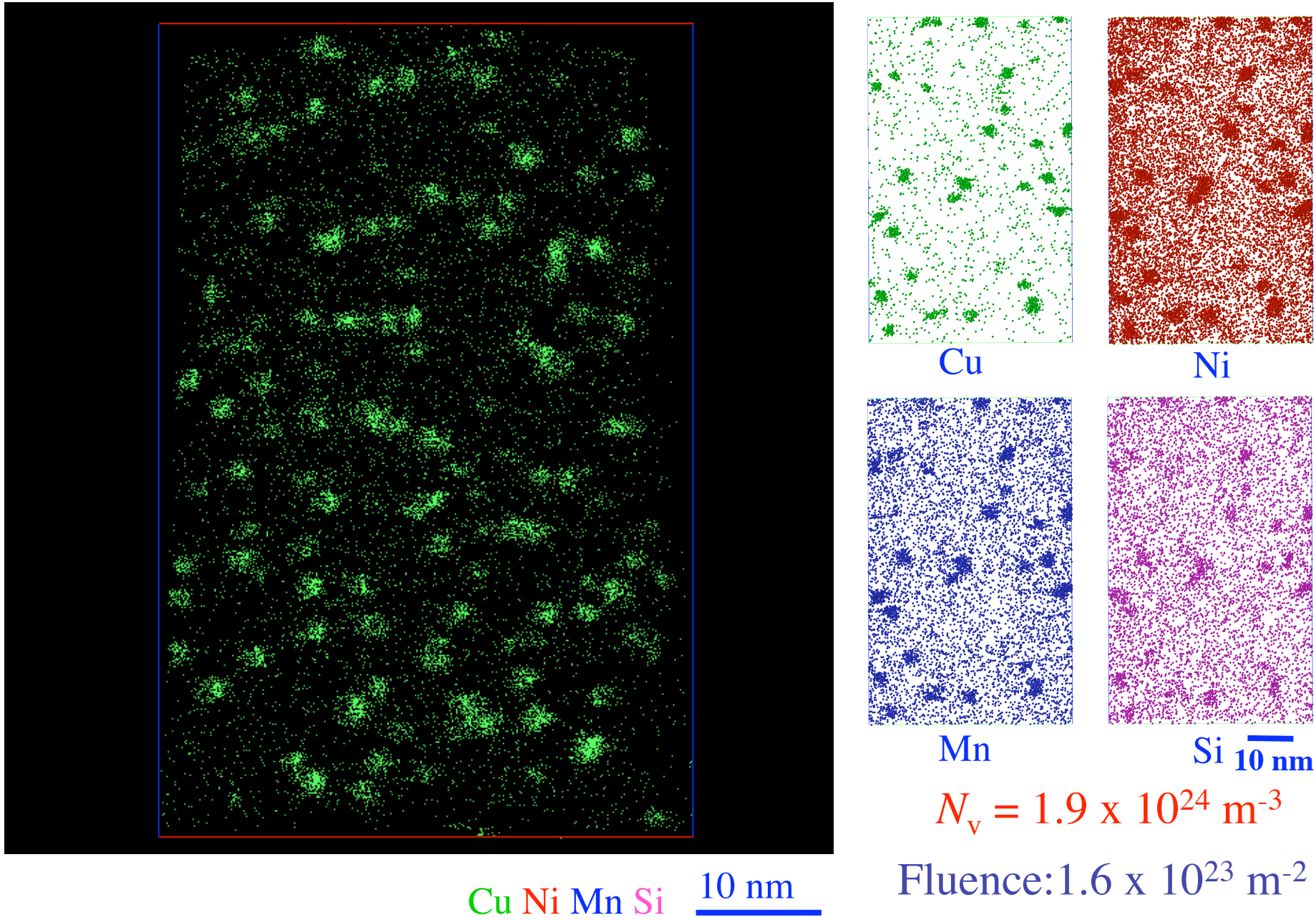
Typical cylinder volume $\approx 50\text{-}100 \text{ nm diameter} \times 100\text{-}500 \text{ nm long}$

CMSX-4 Superalloy

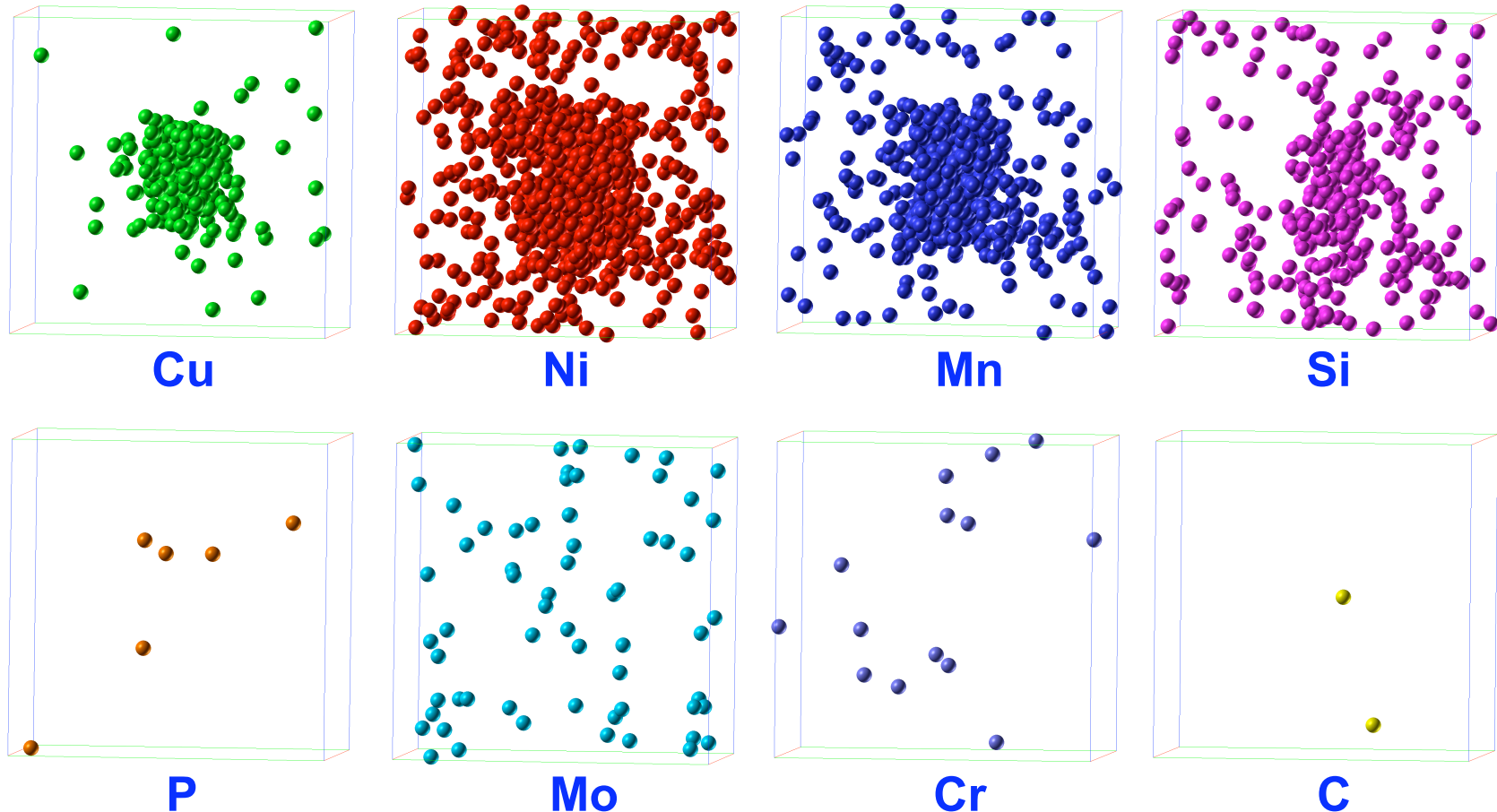


CMSX-4 nickel based superalloy - a precipitate free zone for the the spherical secondary γ' precipitates in the γ channels between the cuboidal primary γ' precipitates

Ultrafine Precipitates in Irradiated Steel



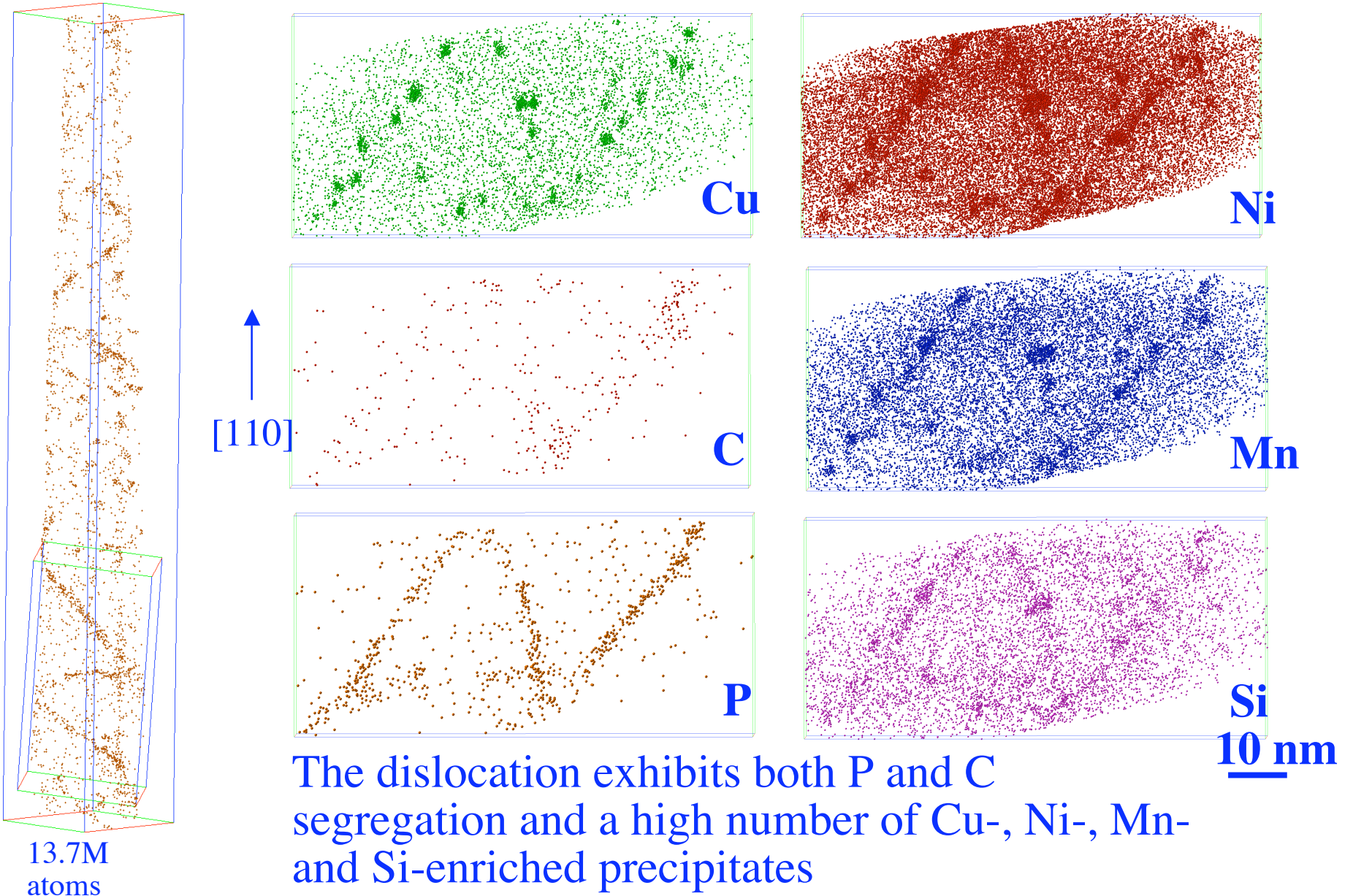
Nanoscale Solute Distribution

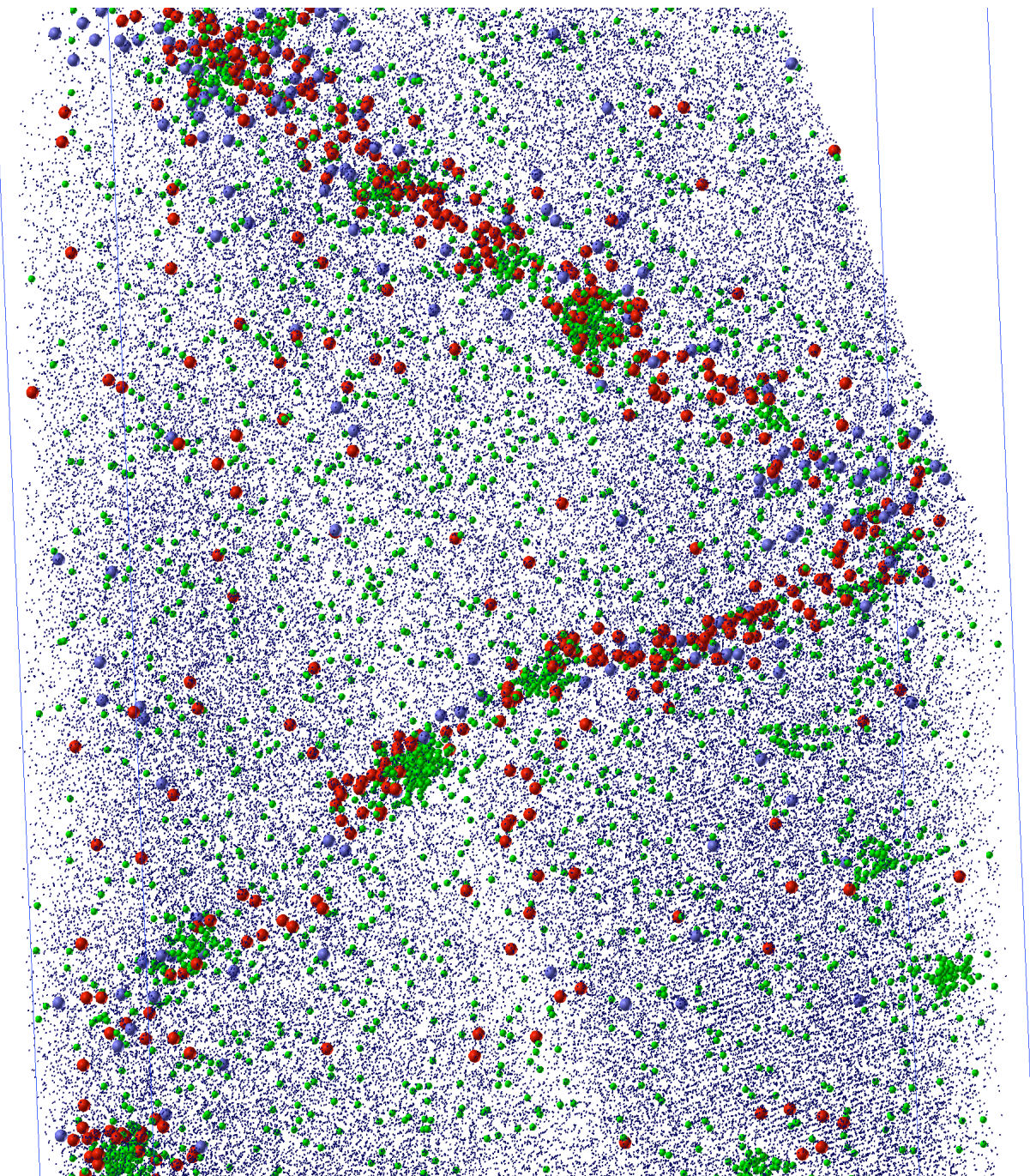


Ni, Mn and Si extents are larger than that of Cu.

Matrix: 0.09at.% Cu, 1.34% Ni, 0.96% Mn, 0.1% Mo, 0.013% P, 0.008% C

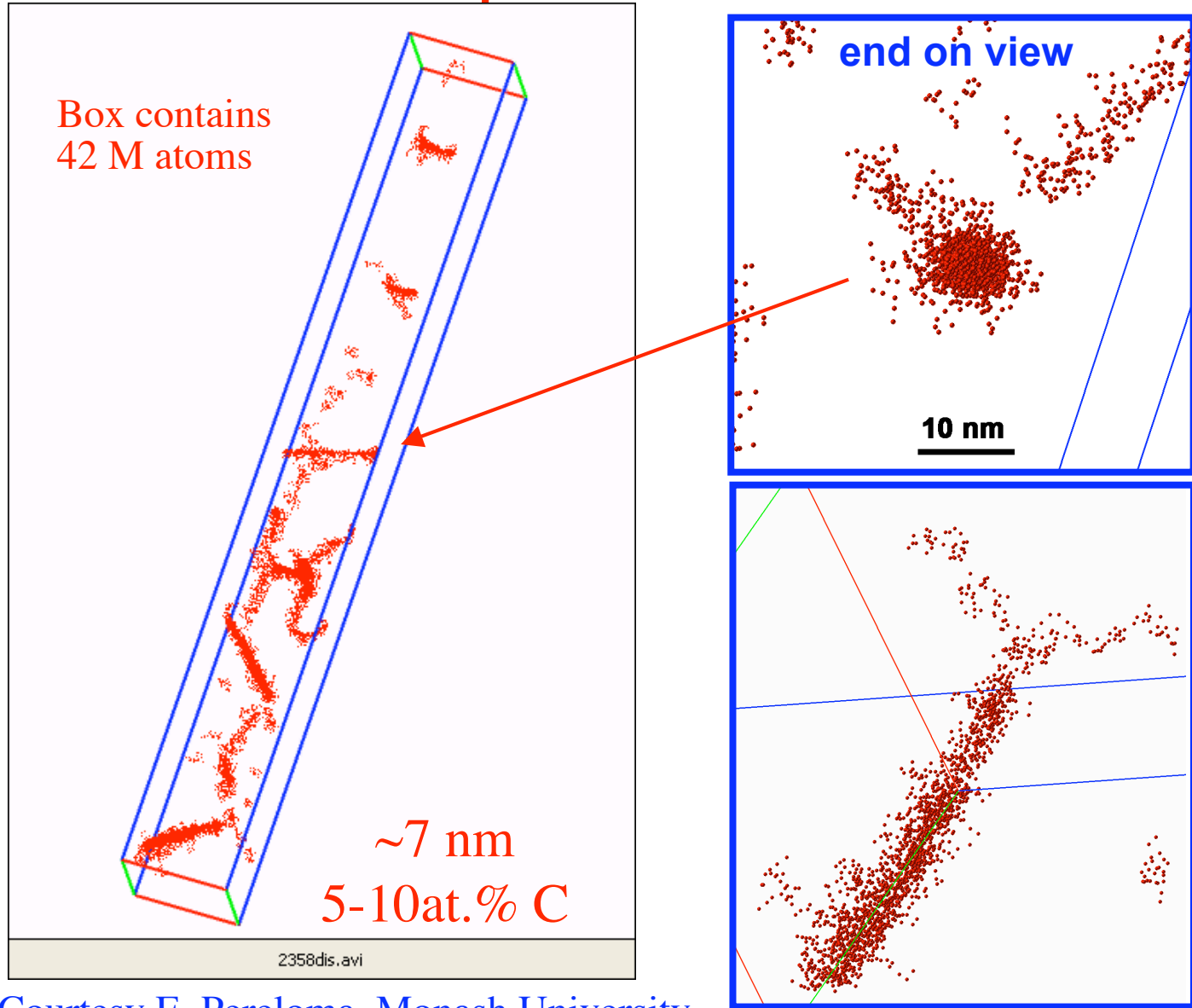
Dislocation in an Irradiated RPV Weld





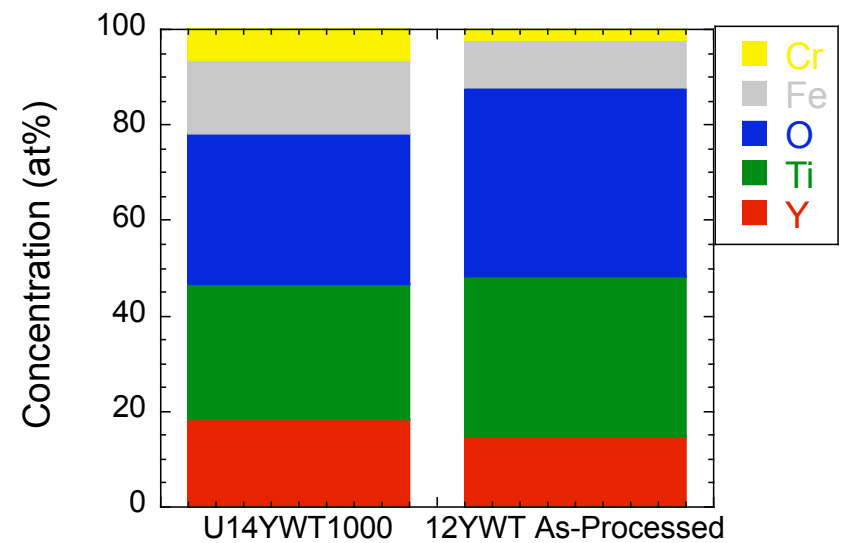
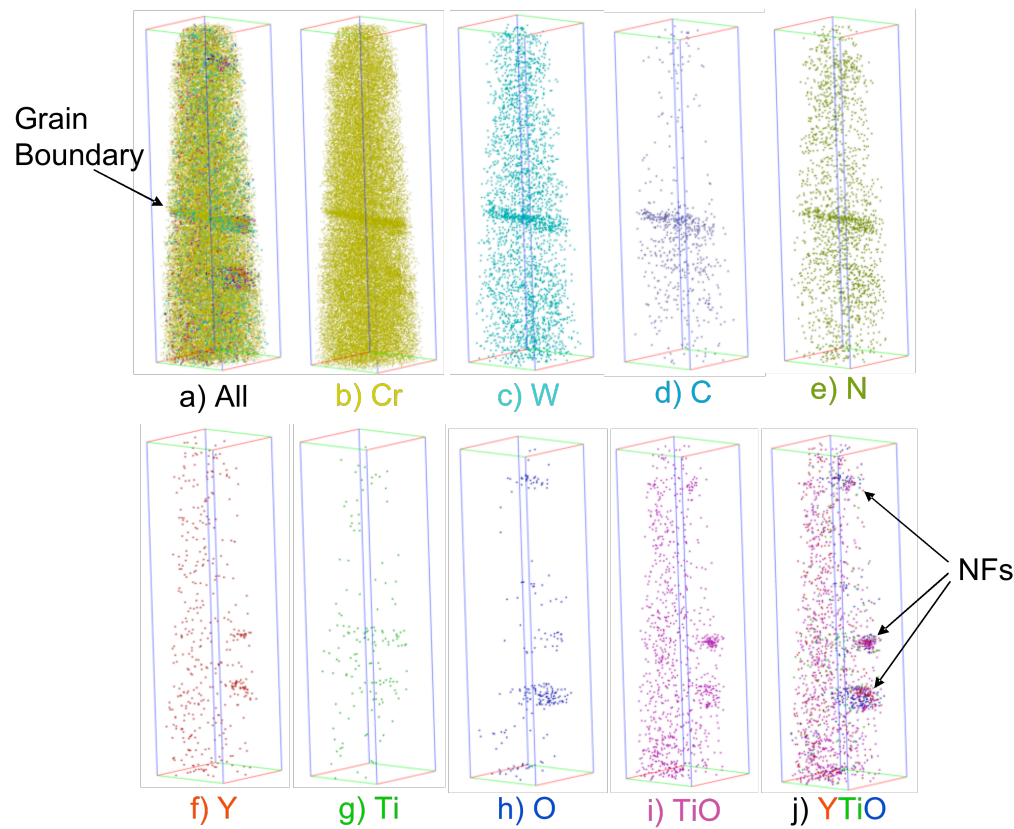
Cottrell Atmospheres in Steel

Red dot is a carbon atom
Other atoms omitted for clarity
Carbon segregation to dislocations evident



Courtesy E. Pereloma, Monash University
Fe 0.039 wt% C, 0.5% Cr, 0.32% Mn, 0.04% P

APT of NFA NC



$Y_2Ti_2O_7$ and $Y_2TiO_5 \rightarrow Y+Ti/O: 4/7$ and $3/5$ $Y/T: 1/1$ and $2/1$

APT $\rightarrow Y+Ti/O: 3/2$ to $1/1$ and $Y/Ti: < 2/3$